Paper

QUANTIFICATION OF RF-EXPOSURE OF THE FETUS USING ANATOMICAL CAD-MODELS IN THREE DIFFERENT GESTATIONAL STAGES

Eugenia Cabot,* Andreas Christ,* Barbara Bühlmann,* Marcel Zefferer,* Nicolas Chavannes,† Jurriaan F. Bakker,‡ Gerard C. van Rhoon,‡ and Niels Kuster*§

Abstract—**This study analyzes the exposure of pregnant women and their fetuses in three different gestational stages to electromagnetic radiation in the radio frequency range in the near- and the far-field using numerical modeling. For far-field exposure, the power density at which the basic restriction for the whole body SAR is reached is calculated for both the mother and the fetus at whole body resonance and at frequencies between 450 MHz and 2,450 MHz. The near-field exposure is assessed at 450 MHz, 900 MHz, and 2,450 MHz using half wavelength dipoles as generic sources located at different locations around the abdomen of the mother. For the investigated cases, the exposure of the mother is always below or on the order of magnitude of the basic restriction for exposure at the reference level. When applying the reference levels for the general public, the fetus is sufficiently shielded by the mother. However, the basic restrictions for general public exposure can be exceeded in the fetus when the mother is exposed at reference levels for occupational conditions. For plane wave exposure at occupational levels, the whole body SAR in the fetus can exceed the basic restrictions for the general population by at least 1.8 dB, and in the near-field of professional devices, the 10 g SAR can be non-compliant with the product standard for the general public by > 3.5 dB.**
Health Phys. 107(5):369–381; 2014

Key words: adsorption; dose assessment; dosimetry; exposure, prenatal

INTRODUCTION

Safety standards for the protection from radio frequency (RF) electromagnetic fields define basic restrictions on whole body and local exposure in terms of the specific absorption rate (SAR) (ICNIRP 1998; IEEE 2005). Limits have been defined for the whole-body average SAR (wbSAR) and peak spatial SAR averaged over 10 g (psSAR10g) or over 1 g (psSAR1g). Their experimental assessment is generally complex and not viable in most practical situations. The standards therefore define reference levels or action values for the incident field at which the basic restrictions are intrinsically met. Different levels of exposure are defined for the general public in uncontrolled environments and for occupational conditions. The latter limits are higher by 5 or 7 dB because exposed personnel are instructed about exposure to the fields and about measures to minimize exposure. Furthermore, workers are healthier than the weakest members of the general public. The correlation of basic restrictions and reference levels used in ICNIRP 1998 and IEEE 2005 is based on greatly simplified models of the human body. While these models can, for example, predict whole body exposure conservatively in most cases (Wang et al. 2006; Dimbylow and Bolch 2007; Nagaoka et al. 2008; Conil et al. 2008), they cannot be used to quantify the induced fields in the fetus in the womb.

A number of numerical studies have been performed to assess the exposure of the mother and the fetus to RF electromagnetic fields in the far-field (plane wave) (Nagaoka et al. 2007; Dimbylow 2007; Bibin et al. 2009; Dimbylow et al. 2009; Kawai et al. 2010) using both anatomical and generic or stylized models integrated into anatomical models of the mother. Only one study (Togashi et al. 2008) analyzes the exposure of the fetus in the immediate environment of an RF transmitter. Table 1 summarizes the characteristics of the fetus models and the investigated scenarios of the cited work.

In Nagaoka et al. (2007), a model of a pregnant woman in the 26th gestational week was presented, as well as the estimation of the whole body averaged SAR in the woman and fetus exposed to vertically and horizontally polarized plane waves in a frequency range from 10 MHz to 2 GHz. For maximum exposure (frontal incidence, vertical E-field vector), the wbSAR of the mother reaches values between 20 mW kg^{-1} W^{-1} m^2 and 30 mW kg^{-1} W^{-1} m^2 at the resonance frequency of the body (about 80 MHz). Under these

*Foundation for Research on Information Technologies in Society (IT'IS), Zeughausstr. 43, 8004 Zürich, Switzerland; †Schmid & Partner Engineering AG (SPEAG), Zeughausstr. 43, 8004 Zürich, Switzerland; ‡Erasmus MC-Daniel den Hoed Cancer Center, Department of Radiation Oncology, Section Hyperthermia, PO box 5201, NL-3008 AE, Rotterdam, The Netherlands; §ETH Zürich, 8092 Zürich, Switzerland.

The authors declare no conflicts of interest.

For correspondence contact: Eugenia Cabot, Foundation for Research on Information Technologies in Society (IT'IS), Zeughausstr. 43, CH-8004, Zürich, Switzerland, or email at **cabot@itis.ethz.ch**.

(*Manuscript accepted* 11 *March* 2014)
0017-9078/14/0
Copyright © 2014 Health Physics Society

DOI: 10.1097/HP.0000000000000129

Copyright © 2014 Health Physics Society. Unauthorized reproduction of this article is prohibited.

Table 1. Summary of studies on the RF exposure of the fetus.

			Fetus model			Exposure	
Reference	Model type	Age	Tissues	Image source	Resolution	RF source	Frequency range
Nagaoka et al. (2007)	Anatomical	26th week	Eyes, brain, body	MR	2 mm	Plane wave	10 MHz–2 GHz
Dimbylow (2007)	Stylized	8th – 36th week	Brain, body, skeleton, soft tissue	—	2 mm	Plane wave	20 MHz–3 GHz
Togashi et al. (2008)	See Nagaoka et al. (2007)					Dipoles at 40mm, generic phone at 10mm distance	900 MHz–2 GHz
Bibin et al. (2009)	Anatomical	30th – 34th week	Not indicated	MR	CAD model	Plane wave	900 MHz
Dimbylow et al. (2009)	Anatomical Additional models from Dimbylow and Bolch (2007), Nagaoka et al. (2007)	13th – 38th week	Brain, skeleton, soft tissue	CT (Xu et al. 2007)	CAD model	Plane wave	20 MHz–3 GHz
Kawai et al. (2010)	stylized	4th and 8th week	Bulk tissue	—	2 mm	Plane wave	10 MHz–1.5 GHz

conditions, the exposure of the fetus is reported to be approximately 50% of the exposure of the mother. For higher frequencies (2 GHz), the wbSAR of the mother drops to about 6 mW kg^{-1} W^{-1} m^2, and the whole body exposure of the fetus reaches approximately 10% of this exposure because of the reduced penetration depth.

In Dimbylow et al. (2009), a comparison of the fetal exposure to plane waves in three sets of models [hybrid mathematical representation of the fetus in the 8th, 13th, 26th, and 38th gestational week; the 26-wk-old model in Nagaoka et al. (2007); and a third anatomical model at 13, 26 and 38 weeks of pregnancy (Xu et al. 2007)] was made for vertical polarization and frontal, back and two sides incidence, from 20 MHz to 3 GHz.** The resonance frequency of the body of the mother (about 80 MHz) lies in the order of magnitude of 30 mW kg^{-1} W^{-1} m^2. The exposure of the different fetus models at this frequency ranges from 7 mW kg^{-1} W^{-1} m^2 to 15 mW kg^{-1} W^{-1} m^2. For increasing frequencies, these values drop with similar characteristics as observed in Nagaoka et al. (2007). Dimbylow et al. (2009) compare whole body as well as localized SAR averaged over 10 g of contiguous tissue. At resonance, it is found to be highest in the stylized model, whereas an additional maximum is observed at 900 MHz for one of the two anatomical models. The authors attribute this to the tissue distribution at the surface of the body. For exposure at the reference levels, however, the localized SAR averaged over 10 g assessed for this model will lie about 10 dB or more below the basic restriction of 2 W kg^{-1}.

Bibin et al. (2009) developed five models (homogeneous mother and heterogeneous fetus) at different gestational ages ranging from the 30th to the 34th week. The models were exposed to a plane wave vertically polarized at 900 MHz. Whole body SAR values of 1 mW kg^{-1} W^{-1} m^2 to 2 mW kg^{-1} W^{-1} m^2 are reported for the fetus, corresponding to approximately 15% to 30% of the whole body SAR of the mother. The psSAR10g of the fetus was found to be more than 15 dB below the basic restriction of 2 W kg^{-1} for plane wave exposure at the reference level. Kawai et al. (2010) presented the calculated dosimetry in 4- and 8-wk-pregnant models exposed to plane waves over the range 10 MHz to 1.5 GHz. Because of the small size of the embryo in these early stages of pregnancy, stylized shapes of only a few mesh cells in size were used for its numerical representation. Up to a frequency of 300 MHz, the whole body absorption in the embryo models compares well to the values reported in Dimbylow (2007) for a stylized model. For higher frequencies, the direction of incidence and the position of the embryo in the womb have a pronounced impact on the absorption.

Little work has been published so far with respect to near-field exposure. The authors of Togashi et al. (2008) used the model in gestational week 26 developed in Nagaoka et al. (2007) to assess the absorption in the fetus and its brain exposed to a half-wave dipole antenna at 900 MHz and 2 GHz at different positions in front of the mother's abdomen at a distance of 40 mm from the skin and for a generic phone model with an integrated antenna placed at one position at a distance of 10 mm. The SAR is

**Dimbylow et al. (2009) revisits the results of the earlier publication (Dimbylow 2007) by the same research group.

Copyright © 2014 Health Physics Society. Unauthorized reproduction of this article is prohibited.

reported as average over all tissues of the fetus (wbSAR of the fetus), as average over its brain only, and as average over the tissues of the mother (wbSAR of the mother). For a radiated power of 1 W, the basic restrictions on the whole body exposure are not violated for any of the cases. The psSAR averaged over 1 g or 10 g of tissue mass, which is generally used to quantify local absorption, is not reported, rendering the interpretation of the results of this study difficult.

All the cited publications conclude that the fetus is sufficiently shielded by the mother, such that the basic restrictions are not violated for exposure of the mother at the reference level under far-field-like conditions. In spite of the large differences of the models used in these studies, the results agree well with respect to their order of magnitude.

OBJECTIVES

The main motivation for the research work in the field of prenatal dosimetry is the higher sensitivity in particular of the unborn child to various kinds of hazardous agents. Several government agencies emphasize this regarding children in general and recommend a precautionary approach, pointing out the need for further research (Kheifets et al. 2005). A prerequisite for the assessment of a possible health risk is a rigorous dosimetric analysis of the exposure of the fetus using highly detailed anatomical models considering a large number of different exposure conditions. Although the anatomical models used in previous studies (Table 1) yield a high level of geometrical detail, they generally distinguish only a small number of fetal tissues. Peak spatial average SAR has not yet been evaluated rigorously for exposure of the abdomen of the pregnant woman to the near-field of RF transmitters. The objectives of this study are therefore:

- the development of highly detailed anatomical CAD models of a pregnant woman in different gestational phases distinguishing at least 15 different tissues and organs of the fetus;
- quantification of the whole body exposure under far-field conditions, under whole-body resonance conditions, and at frequencies of relevant exposure sources, such as exposure to cell towers (e.g., GSM, TETRA);
- characterization of the local absorption of the mother and the fetus at frequencies of relevant exposure sources (e.g., WLAN, Bluetooth);
- evaluation of the numerical uncertainty and assessment of the variability of the results considering, for example, uncertainties and age dependencies of the tissue dielectrics and numerical parameters, such as the mesh resolution; and
- discussion of the results with respect to the exposure limits defined by ICNIRP (1998) and IEEE (2005).

MATERIALS AND METHODS

Anatomical Models of Pregnant Women

Images of whole body scans of pregnant women are difficult to obtain due to ethical reasons. The fetus models therefore had to be developed beforehand and then integrated into an existing female model modified according to the three different gestational ages. For the development of the fetus models, different available resources were used; namely, literature on the anatomy of the fetus and MR and CT scans of the abdomen of a pregnant woman and of a neonate (Veit et al. 1989; Petoussi-Henss et al. 2002). The fetuses could be integrated into the female adult model "Ella" of the Virtual Family (Christ et al. 2010b). Approximately 80 different tissue types were identified and segmented for the mother and about 15 to 17 tissue types for the fetus. The tissues and organs of the fetus models as well as their body masses are given in Table 2. The models were constructed using iSeg (Neufeld 2008) and SEMCAD X 14.2, applying the techniques that had already been used for the development of the Virtual Family (Christ et al. 2010b). More details on the models and their development can be found in Christ et al. (2010c). Fig. 1 shows the anatomical fetus models and their inner organs. The surfaces and the positions of the fetuses of the mother models in the three gestational phases are shown in Fig. 2.

Dielectric tissue parameters

The dielectric parameters of human tissue are compiled in a database for a frequency range from 10 Hz to 100 GHz (Gabriel 1996). They are based on the Cole-Cole dispersion

Table 2. Segmented tissues, organs, and total body mass of the three fetus models.

Tissue	3rd month	7th month	9th month
Bladder	×	×	×
Bone	×	×	×
Brain	×	×	×
Eyes	×	×	×
Fat	×	×	×
Gall bladder		×	×
Heart	×	×	×
Intestine	×	×	×
Kidney	×	×	×
Liver	×	×	×
Lung	×	×	×
Muscle	×	×	×
Subcutaneous adipose tissue		×	×
Skin	×	×	×
Spinal cord	×	×	×
Spleen	×	×	×
Stomach	×	×	×
Mass	15 g	1,700 g	2,700 g

Copyright © 2014 Health Physics Society. Unauthorized reproduction of this article is prohibited.



Fig. 1. Inner organs and skin surface of the three fetus models.

model (Cole and Cole 1941), and appropriate parameters were derived from measurements of animal and human tissue (Gabriel et al. 1996). This database has been applied widely in numerical dosimetry of electromagnetic fields (Hand et al. 2008). Nevertheless, concerns have been raised regarding the applicability of these data for the simulation of children because of possible age-dependent changes in total body water (Anderson 2003; Wang and Fujiwara 2003), and several publications report an increased conductivity in tissues of younger samples (Thurai et al. 1984, 1985; Peyman et al. 2001; Gabriel 2005; Schmid and Uberbacher 2005). A systematic analysis containing the most relevant tissues reported a significant increase in the conductivity and permittivity of tissues with low water content (e.g., skull, bone marrow, or fat) for younger age groups (Peyman et al. 2009), and a study using these data showed a strong impact of the age-dependent changes on the local psSAR10g averaged over bone marrow only, whereas the peak spatial average SAR averaged over all tissues is barely affected (Christ et al. 2010a).

For the current study, the following considerations were taken into account with respect to the tissue parameters:

- Age-dependent parameters of the youngest age groups reported in Schmid and Uberbacher (2005) and Peyman et al. (2009) were used wherever applicable;
- Bone was modeled as bone marrow (properties of skull tissue are reported in Peyman et al. 2009);
- Grey matter was used for the entire brain because of the incomplete myelination of the brain of the fetus (van der Knaap and Valk 1995);
- Placenta and umbilical cord were modeled as blood because of the high perfusion of these tissues; and
- For the remaining tissues, the Cole-Cole model was used (Gabriel et al. 1996).

The impact of the age-dependent dielectric changes of the tissue parameters is considered as a contribution to the uncertainty budget (see Table A1 in the Appendix). The applied tolerance is larger than the changes reported by Peyman et al. (2009).

Numerical simulations

The numerical simulations were performed with the finite-difference time-domain method (FDTD) (Taflove and Hagness 2000), one of the most widely used methods for the modeling of the interaction between non-ionizing electromagnetic fields and the human body (Hand et al. 2008). For the numerical dosimetry of the aforementioned models of a pregnant woman in three gestational ages, far-field and near-field exposures were considered. First, the models were exposed to plane waves with frontal incidence and vertically polarized E-fields at several frequencies under ungrounded conditions (resonance, 450 MHz,

Copyright © 2014 Health Physics Society. Unauthorized reproduction of this article is prohibited.

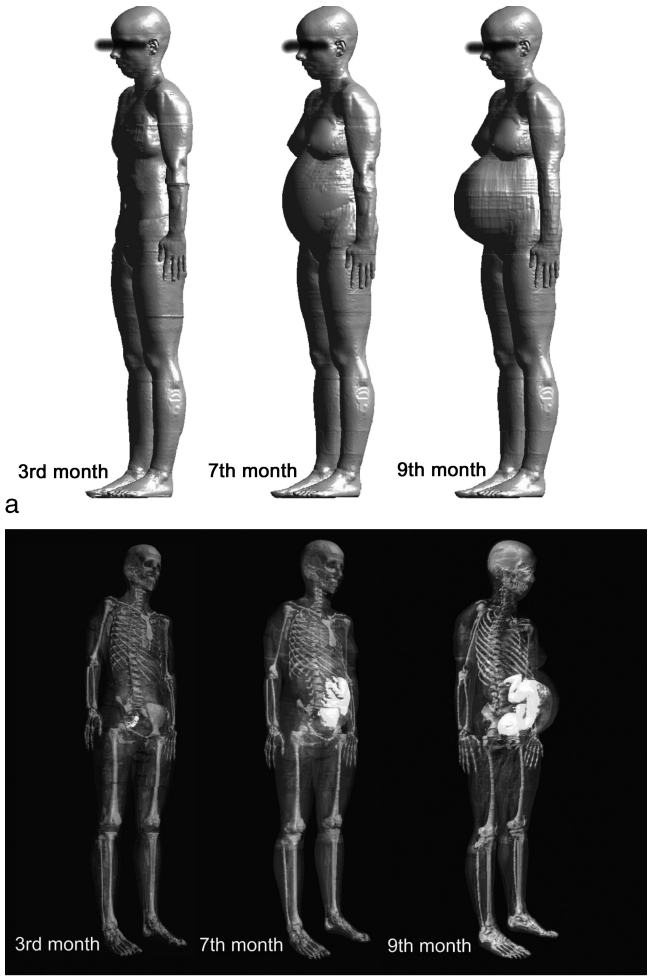


Fig. 2. Anatomical models of the pregnant woman (a) and position of the fetus models in the womb (b).

900 MHz, 1,800 MHz, and 2,450 MHz). Additional simulations were then run with the models exposed to half wavelength dipole antennas at three different frequencies (450 MHz, 900 MHz, and 2,450 MHz). The antennas were positioned at two distances from the model (10 mm and 25 mm) and distributed in 15 different locations in front of the abdominal region. The exact positioning will be explained in the following sections. All the simulations were performed with the FDTD solver SEMCAD X 14.2 (Schmid & Partner Engineering, Zürich). An uncertainty and variability study of the simulations was performed and is presented in the Appendix.

RESULTS

Far-field exposure

The whole body SARs of the mother and of the fetus were evaluated for far-field conditions assuming frontal incidence with the E-field vector oriented parallel to the body axis. Several studies have shown that this condition yields the maximum whole body SAR with respect to the power density of the incident field (Guy and Chou 1986; Dimbylow and Gandhi 1991; Findlay and Dimbylow 2005; Wang et al. 2006; Dimbylow and Bolch 2007; Nagaoka et al. 2008; Conil et al. 2008). The wbSAR was evaluated at the whole body resonance frequency (ungrounded conditions) and at 450 MHz, 900 MHz, 1,800 MHz, and 2,450 MHz. Ungrounded conditions were used at resonance because the exposure in the center of the model (i.e., the abdominal region) can be assumed to be higher than for grounded conditions where the highest exposure occurs in the calves and the feet. The resonance frequencies for the female models were determined by evaluating the whole body SAR in steps of 5 MHz in the expected frequency range (Christ et al. 2009). The body height of the model in the third gestational month is different from the height of the models in the seventh and the ninth months because the abdominal range was replaced in the latter two, as explained in Christ et al. (2010c). A resonance frequency of 70 MHz was determined for the model in the third gestational month and 75 MHz for the other two.

The reference levels for whole body exposure for the frequencies listed above are given in Table 3. The basic restrictions of the whole body SAR are 0.08 W kg^{-1} for uncontrolled exposure and 0.4 W kg^{-1} for occupational exposure (ICNIRP 1998). Table 4 shows the whole body SAR in the mother and in the fetus of the three models normalized to the power density of the incident field. At the resonance frequency of the body of the mother (70 or 75 MHz), the wbSAR of the mother ranges from 29 to 33 mW kg^{-1} W^{-1} m^2 (Table 4), and the exposure of the different fetus models at this frequency ranges from 8.9 to 12 mW kg^{-1} W^{-1} m^2. For increasing frequencies, these values drop with similar characteristics as observed in Nagaoka et al. (2007) and Dimbylow et al. (2009). The values of the wbSAR summarized in Table 4 are generally in good agreement with most of the work discussed in the introduction.

In the frequency range of interest, the reference value of the power density changes significantly with frequency (Table 3). In order to quantify the exposure with respect to the basic restrictions, the power density is calculated at which the whole body SAR limit for the mother and for the fetus is reached. This is shown in Fig. 3, where the

Table 3. Reference levels for the incident power density for exposure of the general public and in occupational environments according to ICNIRP (1998).

Freq. (MHz)	General public (W m^{-2})	Occupational (W m^{-2})
70 and 75	2	10
450	2.25	11.25
900	4.50	22.50
1,800	9	45
2,450	10	50

Copyright © 2014 Health Physics Society. Unauthorized reproduction of this article is prohibited.

Table 4. Whole body SAR in the fetus and in the mother (without amniotic fluid) for plane wave exposure normalized to the incident power density under frontal incidence and orientation of the E-field vector parallel to the vertical axis of the model.

	Fetus wbSAR (mW kg^{-1} W^{-1} m^2)			Mother wbSAR (mW kg^{-1} W^{-1} m^2)		
Freq. (MHz)	3 mo	7 mo	9 mo	3 mo	7 mo	9 mo
70 and 75	11.4	12	8.9	33	29	30
450	0.34	4.9	2.7	7.7	7.9	8
900	0.46	3.3	2.8	8.6	7.5	7.5
1,800	0.03	1.4	2	7	5.9	6.1
2,450	0.003	0.7	1.9	5.7	4.7	4.8

power density to reach the SAR limit is displayed normalized to the reference level of the incident field.

For all investigated cases, the whole body SAR of the mother does not reach the basic restrictions for exposure at the reference level if either occupational or uncontrolled limits are applied. At resonance frequency and at 1,800 MHz and 2,450 MHz, however, it is only 1 dB to 3 dB below the basic restrictions. In general, the reference levels are conservative with respect to the basic restrictions for the mother, which have already been confirmed in similar studies where violations were only reported for young children at resonance frequency and in the frequency range from 1.5 GHz to 5 GHz (Wang et al. 2006; Dimbylow and Bolch 2007; Nagaoka et al. 2008; Conil et al. 2008; Kuhn et al. 2009). The whole body SAR in the fetus model lies significantly below the exposure limits. Maximum exposure occurs at resonance (5–7 dB below the exposure limits) for all models. At higher frequencies, the exposure of the 3-mo-old fetus is significantly lower because of the decreased penetration depth. For the older fetus models, it lies between 7 dB and 12 dB below the exposure limits.

For occupational exposure levels for the incident field, violations of the basic restrictions for the fetus on the whole body SAR under uncontrolled conditions can be observed in several cases. For exposure at the whole body resonance frequency of the mother (ungrounded) at a power density of 10 W m^{-2} (Table 3), the basic restriction of the whole body SAR of 0.08 W kg^{-1} is exceeded by 0.5 dB to 1.8 dB for all three gestational phases. For the 9-mo-old fetus, this was also observed at 1,800 MHz and 2,450 MHz because the position of this model is comparatively close to the surface of the abdomen of the mother [this finding supports the work of Dimbylow et al. (2009) for higher frequencies and later gestational stages]. The exposure exceeds the basic restrictions by 0.5 dB to 0.6 dB. These cases are marked with an asterisk in Fig. 3. The uncertainty of the whole body exposure has been assessed as 1.1 dB for the mother and as 3.7 dB for the fetus models (Tables A5 and A6 of the Appendix).

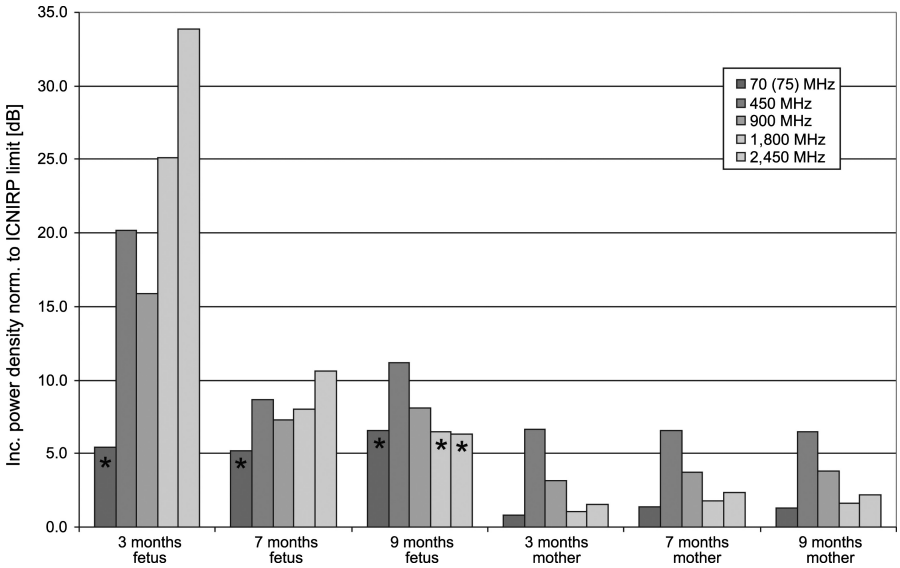


Fig. 3. Incident power density (in dB above the ICNIRP limit, Table 3) required to reach the whole body SAR level of the basic restrictions of 0.4 W kg^{-1} (occupational) or 0.08 W kg^{-1}. Since both reference levels and basic restrictions scale by a factor of 5, the graph applies to both occupational and uncontrolled exposure. The asterisks indicate those cases where the whole body exposure limit for uncontrolled environments is exceeded for the fetus if the mother is exposed at the reference levels for occupational conditions

Copyright © 2014 Health Physics Society. Unauthorized reproduction of this article is prohibited.

In summary, the reference levels can be considered as conservative with respect to the basic restrictions for whole body exposure of both the mother and the fetus if either occupational or uncontrolled limits apply. Although the exposure of the fetus is generally well under the limits (>5 dB), the exposure of the mother has a comparatively low safety margin of 0.8 dB at resonance and about 1 dB to 2 dB for the higher frequencies (Fig. 3). As observed in related studies on whole body exposure, this safety margin depends strongly on body height and weight, and reference levels are generally not conservative for young children (Wang et al. 2006; Dimbylow and Bolch 2007; Nagaoka et al. 2008; Conil et al. 2008; Kuhn et al. 2009; Bakker et al. 2010, 2011). For exposure of the mother at occupational reference levels, however, the exposure of the fetus can exceed the basic restrictions for uncontrolled exposure by up to 1.8 dB for the investigated pregnant models. The worst-case exposure could be higher, as the induced fields in the abdomen depend on the anatomical features of the mother.

Near-field exposure in the immediate environment of the abdomen

The exposure in the immediate near-field (e.g., due to wireless devices worn or operated on the body) was assessed using half wavelength dipole antennas as generic exposure sources. The antennas were placed in front of the abdomen in a matrix of three rows and five angles around the body axis for two distances from the antenna feedpoint to the body (10 mm and 25 mm). In all positions, the antennas were aligned tangentially to the closest point of the body. Fig. 4 shows the positioning of the antennas in front of the abdomen of the mother in the seventh gestational month. The diameter of the dipole antenna models was 3.6 mm. The distances of 10 mm and 25 mm refer to the dipole axes. A distance of 10 mm is considered as a realistic minimum for worst case exposure, taking into account the case of the wireless device, clothing, the antenna diameter, etc. The distance of 25 mm was chosen because of the strong field decay in the immediate environment of the antenna. At 25 mm, the decay of the fields in the tissue is already on the order of magnitude of the free space penetration depth (i.e., the theoretical minimum of decay). Further details on the characteristics of the absorption in the near-field can be found in Kuster and Balzano (1992). A comparison of the near-field penetration of the fields of different portable devices is presented in Kanda et al. (2004). Changes with respect to free space decay have been considered in the uncertainty evaluation of the exposure in the near-field (Appendix).

For the evaluation of the near-field exposure, frequencies of 450 MHz, 900 MHz, and 2,450 MHz were considered. The local exposure was calculated as peak spatial average SAR (psSAR) in a cubical volume of 10 g tissue mass (IEEE 2002). Reference values of the 10 g psSAR calculated for exposure of a flat phantom to the half wavelength dipoles are given in Table 5. The values of psSAR are given for 1 W antenna power, but they would be lower for the usual levels of average output power of GSM or UMTS. The dielectric properties of the flat phantom correspond to those defined as tissue simulants in compliance testing of body-mounted wireless devices (IEC 2007). In the following, the local exposure values of the mother and the fetus models are normalized to these results.

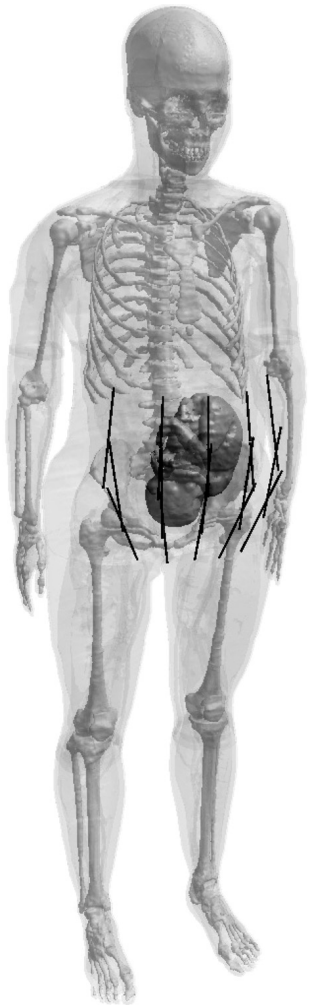


Fig. 4. Woman in the seventh gestational month with half wavelength dipole antennas (900 MHz) in 15 different positions placed at 25 mm distance in front of the abdomen.

Figs. 5–7 show the 10 g psSAR in the fetus and in the mother normalized to the antenna input power (difference of the forward and the reflected power) required to reach the SAR in the flat phantom given in Table 5. The columns indicate the average of the 15 exposure positions, and the error bars indicate the minimum and maximum

Copyright © 2014 Health Physics Society. Unauthorized reproduction of this article is prohibited.

Table 5. 10 g peak spatial average SAR in a phantom irradiated by a half wavelength dipole at 10 mm and 25 mm distance (1 W antenna power) according to the specifications in IEC (2007).

	10 mm		25 mm	
Freq. (MHz)	1 g SAR (W kg^{-1})	10 g SAR (W kg^{-1})	1 g SAR (W kg^{-1})	10 g SAR (W kg^{-1})
450	6.3	4.0	3.7	2.6
900	14.5	8.6	6.1	4.1
2,450	53.6	24.2	6.1	3.3

values observed. With the exception of the model in the ninth gestational month at 450 MHz and 2,450 MHz, the flat phantom is always conservative for the assessment of the exposure of the mother (0 dB to 10 dB of overestimation). At 2,450 MHz, it can underestimate the 10 g psSAR by up to 2.5 dB. This is due to the particular tissue distribution in the abdomen of the mother: the layer of lossy skin and subcutaneous tissue is comparatively thin. The cubical volume of 10 g tissue mass therefore contains a significant amount of air and amniotic fluid, which is not considered as tissue for the calculation of the psSAR. The psSAR is therefore averaged over a comparatively large and flat patch of skin, whereas the psSAR in the flat phantom is calculated over a cubic volume filled entirely with tissue simulant. The SAR decays rapidly in the flat phantom, whereas it remains high at the surface. A situation like this would be appropriately considered by averaging the SAR over a contiguous volume, as suggested in ICNIRP (1998).

The psSAR of the fetus is generally lower. For the 3-mo-old fetus, a value of −20 dB below the psSAR of the flat phantom is never exceeded. For the 7- and 9-mo-old models, the exposure can reach values of up to −3.5 dB below the psSAR of the flat phantom (Fig. 7, 450 MHz, 10 mm distance). For cases where the exposure is higher than −7 dB below the psSAR of the flat phantom, the basic restriction for the general public can be exceeded for the fetus if occupational SAR limits apply to the mother. The numerical uncertainty of the individual values presented here was assessed as 3.3 dB for the fetus and 5.3 dB for the mother (Tables A1 and A3 of the Appendix).

The variability of the local exposure considering the different sizes and positions of the fetus in the womb was assessed as 10.2 dB for the fetus and 7.7 dB for the mother, including the numerical uncertainty (Tables A2 and A4 of the Appendix).

CONCLUSION

The results of far-field and near-field exposure of three pregnant woman models in different gestational stages have been presented. The whole body exposure of the models to frontally incident vertically polarized plane waves at several frequencies has shown that the reference levels can be considered as conservative with respect to

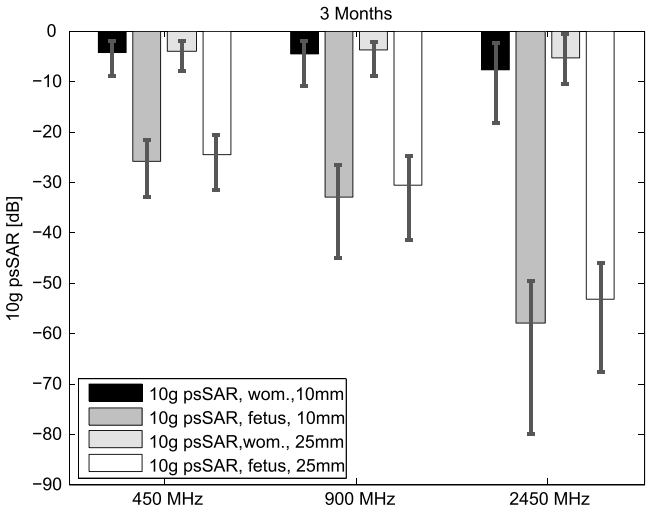


Fig. 5. 10-g peak spatial average SAR of the mother and the whole body SAR in the 3-mo-old fetus for the 15 different positions of the half wavelength dipole at 10 mm and 25 mm distance and at 450 MHz, 900 MHz, and 2,450 MHz normalized to the SAR in a flat phantom (Table 5). The error bars indicate the minimum and maximum value observed.

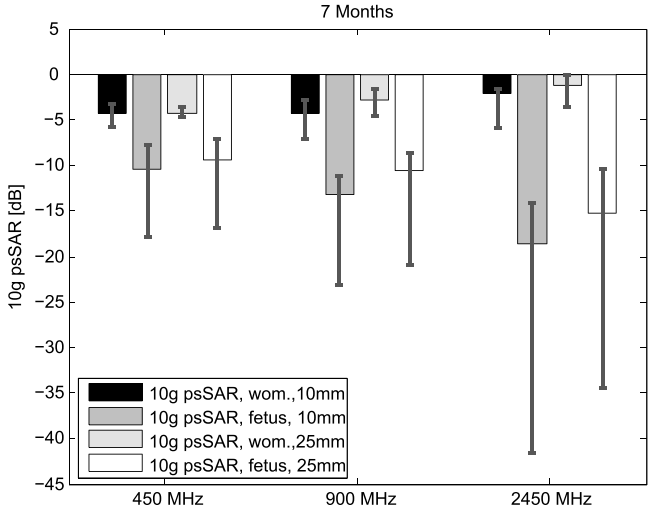


Fig. 6. 10-g peak spatial average SAR of the mother and of the 7-mo-old fetus for the 15 different positions of the half wavelength dipole at 10 mm and 25 mm distance and at 450 MHz, 900 MHz, and 2,450 MHz normalized to the SAR in a flat phantom (Table 5). The error bars indicate the minimum and maximum value observed.

Copyright © 2014 Health Physics Society. Unauthorized reproduction of this article is prohibited.

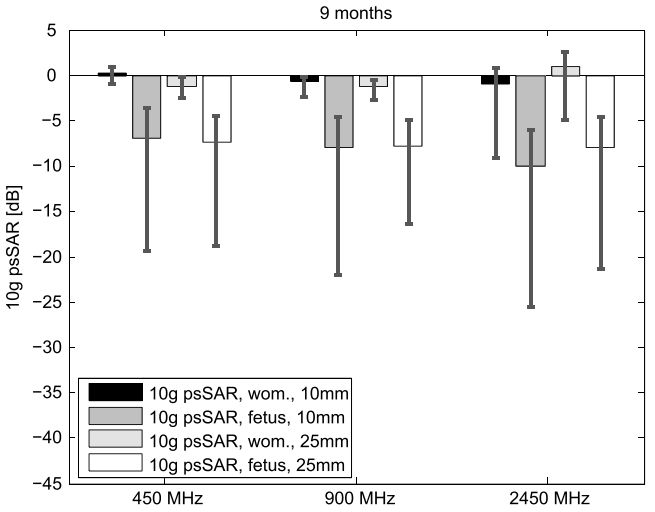


Fig. 7. 10-g peak spatial average SAR of the mother and of the 9-mo-old fetus for the 15 different positions of the half wavelength dipole at 10 mm and 25 mm distance and at 450 MHz, 900 MHz, and 2,450 MHz normalized to the SAR in a flat phantom (Table 5). The error bars indicate the minimum and maximum value observed.

the basic restrictions of both the mother and the fetus if either occupational or uncontrolled limits apply for both the mother and the fetus. The same is true for transmitters operating in closest vicinity to the womb if tested according to today's product standards. However, if the mother is exposed at the acceptable level for occupational exposure, the fetus can be exposed to levels that are >1.8 dB above the basic restrictions for uncontrolled exposure (far-field exposure) and >3.5 dB for body-worn devices. Hence, pregnant women should not be exposed to conditions above the limits for the general public if the fetus is not considered to be a worker.

Acknowledgments—The authors would like to thank the Swiss National Fund (National Research Program 57) and The Netherlands Organization for Health Research and Development (ZonMw) for the financial support of this study. The authors want to express their gratitude to Maria Zankl (Helmholtz Institute, Germany) for providing the anatomical images for the development of the 9-mo fetus model.

REFERENCES

Anderson V. Comparisons of peak SAR levels in concentric sphere head models of children and adults for irradiation by a dipole at 900 MHz. Phys Med Biol 48:3263–3275; 2003.

Bakker JF, Paulides MM, Christ A, Kuster N, van Rhoon GC. Assessment of induced SAR in children exposed to electromagnetic plane waves between 10 MHz and 5.6 GHz. Phys Med Biol 55:3115–3130; 2010.

Bakker JF, Paulides MM, Neufeld E, Christ A, Kuster N, van Rhoon GC. Children and adults exposed to electromagnetic fields at the ICNIRP reference levels: theoretical assessment of the induced peak temperature increase. Phys Med Biol 56:4967–4989; 2011.

Bibin L, Anquez J, Hadjem A, Angelini E, Wiart J, Bloch I. Dosimetry studies on a fetus model combining medical image information and a synthetic woman body. In: World Congress on Medical Physics and Biomedical Engineering. Munich: Springer; 2009:321–324.

Christ A, Schmid G, Djafarzadeh R, Uberbacher R, Cecil S, Zefferer M, Neufeld E, Lichtsteiner M, Bouterfas M, Kuster N. Numerische Bestimmung der Spezifischen Absorptionsrate bei Ganzkorperexposition von Kindern: Abschlussbericht. Zurich, Switzerland: Tech Rep IT'IS Foundation, ETH Zurich, Zeughausstr 43, 8004; 2009 (in German).

Christ A, Gosselin MC, Christopoulou M, Kuhn S, Kuster N. Age-dependent tissue specific exposure of cell phone users. Phys Med Biol 55:1767; 2010a.

Christ A, Kainz K, Hahn E G, Honegger K, Zefferer M, Neufeld E, Rascher W, Janka R, Bautz W, Chen J, Kiefer B, Schmitt P, Hollenbach HP, Shen J, Oberle M, Szczerba D, Kam A, Guag JW, Kuster N. The virtual family—development of surface based anatomical models of two adults and two children for dosimetric simulations. Phys Med Biol 55: N23–N38; 2010b.

Christ A, Buhlmann B, Cabot E, Zefferer M, Gosselin M-C, Kyriacou A, Neufeld E, Chavannes N, Kuster N. Assessment of the exposure of the fetus to electromagnetic fields in uncontrolled environments. Zurich, Switzerland: Tech Rep IT'IS Foundation, ETH Zurich, Zeughausstr 43, 8004; 2010c.

Cole KS, Cole RH. Dispersion and absorption in dielectrics—I. Alternating current characteristics. J Chemical Phys 9: 341–351; 1941.

Conil E, Hadjem A, Lacroux F, Wong M, Wiart J. Variability analysis of SAR from 20 MHz to 2.4 GHz for different adult and child models using finite-difference time-domain. Phys Med Biol 53:1511; 2008.

Dimbylow PJ, Gandhi OP. Finite-difference time-domain calculations of SAR in a realistic heterogeneous model of the head for plane-wave exposure from 600 MHz to 3 GHz. Phys Med Biol 36:1075–1089; 1991.

Dimbylow P. SAR in the mother and foetus for RF plane wave irradiation. Phys Med Biol 52:3791; 2007.

Dimbylow P, Bolch W. Whole-body-averaged SAR from 50 MHz to 4 GHz in the University of Florida child voxel phantoms. Phys Med Biol 52:6639–6650; 2007.

Dimbylow P, Nagaoka T, Xu X. A comparison of foetal SAR in three sets of pregnant female models. Phys Med Biol 54:2755–2767; 2009.

Findlay RP, Dimbylow PJ. Effects of posture on FDTD calculations of specific absorption rate in a voxel model of the human body. Phys Med Biol 50:3825–3835; 2005.

Gabriel C. Compilation of the dielectric properties of body tissues at RF and microwave frequencies. Brooks Air Force Base, TX: Occupational and Environmental Health Directorate, Radiofrequency Radiation Division; Tech Rep, Report N.AL/OE-TR-1996-0037; 1996.

Gabriel S, Lau RW, Gabriel C. The dielectric properties of biological tissues: III. Parametric models for the dielectric spectrum of tissues. Phys Med Biol 41:2271–2293; 1996.

Gabriel C. Dielectric properties of biological tissue: variation with age. Bioelectromagnetics 26:S12–S18; 2005.

Guy AW, Chou CK. Specific absorption rates of energy in man models exposed to cellular UHF mobile-antenna fields. IEEE Trans Microwave Theory Techniques 34:671–680; 1986.

Hand J, Boucek J, Francis R, Jones C, Khan N, Turlach B, Green A. Modelling the interaction of electromagnetic fields (10 MHz–10 GHz) with the human body: methods and applications. Phys Med Biol 53:R243–R286; 2008.

International Commission on Non-Ionizing Radiation Protection. Guidelines for limiting exposure to time-varying electric, magnetic and electromagnetic fields (up to 300 GHz). Health Phys 74:494–522; 1998.

Copyright © 2014 Health Physics Society. Unauthorized reproduction of this article is prohibited.

International Electrotechnical Commission. Human exposure to radio frequency fields from handheld and body-mounted wireless communication devices—human models, instrumentation and procedures, part 2: procedure to determine the specific absorption rate (SAR) for mobile wireless communication devices used in close proximity to the human body (frequency range of 30MHz to 6 GHz), Draft. Geneva, Switzerland: IEC; IEC Technical Committee 106; IEC 62209 Part 2; 2007.

Institute of Electrical and Electronics Engineers. Recommended practice for measurements and computations of radio frequency electromagnetic fields with respect to human exposure to such fields, 100 kHz–300 GHz. New York: International Committee on Electromagnetic Safety, Institute of Electrical and Electronics Engineers, IEEE Standards Department; Std C95.3; 2002.

Institute of Electrical and Electronics Engineers. IEEE standard for safety levels with respect to human exposure to radio frequency electromagnetic fields, 3 kHz to 300 GHz. New York: International Committee on Electromagnetic Safety, The Institute of Electrical and Electronics Engineers, Inc., IEEE Standards Department; SCC28, IEEE Std C95.1–2005; 2005.

Institute of Electrical and Electronics Engineers. Draft recommended practice for determining the spatial-peak specific absorption rate (SAR) in the human body due to wireless communications devices, 30 MHz–6 GHz: general requirements for using the finite difference time domain (FDTD) method for SAR calculations. New York: Tech Rep, Working Group 2 of the ICES TC34/SC2 Committee; 1528.1 D1.0; 2008.

Kanda M, Douglas M, Mendvil E, Ballen M, Gessner A, Chou C. Faster determination of mass-averaged SAR from 2-D area scans. IEEE Trans Microwave Theory Techniques 52: 2013–2020; 2004.

Kawai H, Nagaoka T, Watanabe S, Saito K, Takahashi M, Ito K. Computational dosimetry in embryos exposed to electromagnetic plane waves over the frequency range of 10 MHz–1.5 GHz. Phys Med Biol 55:N1; 2010.

Kheifets L, Repacholi M, Saunders R, van Deventer E. The sensitivity of children to electromagnetic fields. Pediatrics 116:e303–e313; 2005.

Kuhn S, Jennings W, Christ A, Kuster N. Assessment of induced radio-frequency electromagnetic fields in various anatomical human body models. Phys Med Biol 54:875–890; 2009.

Kuster N, Balzano Q. Energy absorption mechanism by biological bodies in the near field of dipole antennas above 300 MHz. IEEE Trans Vehicular Technol 41:17–23; 1992.

Nagaoka T, Togashi T, Saito K, Takahashi M, Ito K, Watanabe S. An anatomically realistic whole-body pregnant-woman model and specific absorption rates for pregnant-woman exposure to electromagnetic plane waves from 10 MHz to 2 GHz. Phys Med Biol 52:6731–6746; 2007.

Nagaoka T, Kunieda E, Watanabe S. Proportion-corrected scaled voxel models for Japanese children and their application to the numerical dosimetry of specific absorption rate for frequencies from 30 MHz to 3 GHz. Phys Med Biol 53: 6695–6711; 2008.

Neufeld E. High resolution hyperthermia treatment planning. Zurich, Switzerland: Swiss Federal Institute of Technology; Diss. ETH Nr. 17947, Defense 19; 2008. Dissertation.

Petoussi-Henss N, Zankl M, Fill U, Regulla D. The GSF family of voxel phantoms. Phys Med Biol 47:89–106; 2002.

Peyman A, Rezazadeh AA, Gabriel C. Changes in the dielectric properties of rat tissue as a function of age at microwave frequencies. Phys Med Biol 46:1617–1629; 2001.

Peyman A, Gabriel C, Grant EH, Vermeeren G, Martens L. Variation of the dielectric properties of tissues with age: the effect on the values of SAR in children when exposed to walkie-talkie devices. Phys Med Biol 54:27–241; 2009.

Schmid G, Uberbacher R. Age dependence of dielectric properties of bovine brain and ocular tissues in the frequency range of 400 MHz to 18 GHz. Phys Med Biol 50:4711; 2005.

Taflove A, Hagness SC. Computational electromagnetics: the finite-difference time-domain method. Boston, London, United Kingdom: Artech House, Inc.; 2000.

Thurai M, Goodridge VD, Sheppard RJ, Grant EH. Variation with age of the dielectric properties of mouse brain cerebrum. Phys Med Biol 29:1133–1136; 1984.

Thurai M, Steel MC, Sheppard RJ, Grant EH. Dielectric properties of developing rabbit brain at 37 degrees. Bioelectromagnetics 6:235–242; 1985.

Togashi T, Nagaoka T, Kikuchi S, Saito K, Watanabe S, Takahashi M, Ito K. FDTD calculations of specific absorption rate in fetus caused by electromagnetic waves from mobile radio terminal using pregnant woman model. IEEE Trans Microwave Theory Techniques 56:554–559; 2008.

van der Knaap MS, Valk J. Magnetic resonance of myelin, myelination and myelin disorder. Berlin: Springer; 1995.

Veit R, Petoussi M, Mannweiler N, Williams E, Drexler G. Tomographic anthropomorphic models, part I: construction technique and description of models of an 8 week old baby and a 7 year old child. Neuherberg, Germany: Tech Rep GSF-Bericht 3/89, GSF Forschungszentrum fur Umwelt und Gesundheit; 1989.

Wang J, Fujiwara O. Comparison and evaluation of electromagnetic absorption characteristics in realistic human head models of adult and children for 900 MHz mobile telephones. IEEE Trans Microwave Theory Techniques 51:966–971; 2003.

Wang J, Fujiwara O, Kodera S, Watanabe S, FDTD calculation of whole-body average SAR in adult and child models for frequencies from 30 MHz to 3 GHz. Phys Med Biol 51:4119–4128; 2006.

Xu X, Taranenko V, Zhang J, Shi C. A boundary-representation method for designing whole-body radiation dosimetry models: pregnant females at the ends of three gestational periods -P3, -P6 and -P9. Phys Med Biol 52:7023–7044; 2007.

■■

Copyright © 2014 Health Physics Society. Unauthorized reproduction of this article is prohibited.

APPENDIX

Uncertainty and variability assessment

The numerical uncertainty and the variability of the exposure of the mother and the fetus have been analyzed separately, distinguishing near-field and far-field exposure. The uncertainty of the local RF exposure is higher than the whole body RF exposure due to the important individual contributions of the variability in position of the source and fetus to the total budget. In addition, the impact of the dielectric parameters of the tissues is also more noticeable in the local exposure. The uncertainty assessment is presented in Tables A1–A5. The analysis follows the procedure outlined in the current draft of (IEEE 2008); additional explanations are given on how the contributions to the total uncertainty were assessed.

Table A1. Numerical uncertainty of the local RF exposure of the fetus.

Uncertainty Source	Tolerance	Distrib.	Div.	c_i	Std. Unc.	Conf. Interval	*veff*
Grid resolution[a]	0.2 dB	normal	1	1	0.2 dB	0.96 – 1.04	∞
Absorbing boundary conditions[b]	0.0 dB	normal	1	1	0.0 dB	1.00	∞
Tissue parameters fetus[c]	0.9 dB	normal	1	1	0.9 dB	0.82 – 1.22	∞
Simulation time[b]	0.0 dB	normal	1	1	0.0 dB	1.00	∞
Tissue parameters mother[c]	0.9 dB	normal	1	1	0.9 dB	0.81 – 1.24	∞
Amniotic fluid[c]	0.6 dB	normal	1	1	0.6 dB	0.87 – 1.15	∞
SAR Averaging[d]	1.3 dB	rect.	√3	1	0.8 dB	0.33 – 3.03	∞
Power budget[e]	0.2 dB	normal	1	1	0.2 dB	0.96 – 1.04	∞
Combined std. uncertainty			RSS		1.5 dB	0.71 – 1.41	
Expanded uncertainty *(k_p = 2)*					**2.6 dB**	0.55 – 1.83	

[a]The grid resolution in the fetus is varied between 0.75 mm and 1.0 mm. Due to the grid topology, these changes also affect the resolution of the mother model. The maximum deviation is reported.

[b]The impact of the simulated time and the spurious reflections of the absorbing boundary conditions was assessed by extending the time by a quarter period and increasing the distance to the boundaries by a quarter wavelength according to the recommendations of IEEE (2008). It is negligible for the settings and configurations used here.

[c]The uncertainty due to the age dependence of the tissue parameters was assessed by replacing the dielectric parameters for the tissue of the unborn, as discussed in section 3.2, by the parameters of the Cole-Cole model. In order to estimate the impact of the parameters of the tissue of the mother, the layer of fat and subcutaneous tissue of the mother's abdomen in the model in the 7th gestational month was replaced by muscle tissue, which has a significantly higher permittivity and conductivity. For the assessment of the impact of the attenuation in the amniotic fluid, its conductivity was increased by 15 %.

[d]For the fetus models, the SAR averaging uncertainty is based on the difference in body mass of the three-month-old model. Here, the 10 g value could not be assessed for technical reasons. The uncertainty can be estimated conservatively by assuming that the entire power is absorbed in a fraction of the body with a mass of 10 g. For the other cases, it is assessed on the basis of the maximum tolerance of the averaging volume as specified in IEEE (2002).

[e]The power budget is the ratio of the sum of the radiated and absorbed powers to the power fed into the computational domain. For plane wave exposure, the power fed into the computational domain cannot be determined. It has therefore been estimated based on simulations with known source power (Christ et al. 2009).

Table A2. Numerical uncertainty and variability of the fetus for local RF exposure.

Uncertainty source	Tolerance	Distrib.	Div.	c_i	Std. unc.	Conf. interval	*veff*
Num. uncertainty (Table A1)	1.60 dB	normal	1	1	1.60 dB	0.71 – 1.41	∞
Device representation[a]	0.25 dB	normal	1	1	0.25 dB	0.95 – 1.06	∞
Position of source and fetus[b]	4.80 dB	normal	1	1	4.80 dB	0.33 – 3.00	15
Combined std. uncertainty			RSS		4.90 dB	0.33 – 3.10	
Expanded uncertainty *(k_p = 2)*					**7.10 dB**	0.19 – 5.10	

[a]The device representation is based on the variability of the field decay reported in Kanda et al. (2004) for a large set of different devices.

[b]The positioning uncertainty was assessed using the standard deviation of the local exposure as evaluated above.

Copyright © 2014 Health Physics Society. Unauthorized reproduction of this article is prohibited.

Table A3. Numerical uncertainty of the local RF exposure of the mother.

Uncertainty source	Tolerance	Distrib.	Div.	*ci*	Std. unc.	Conf. interval	*veff*
Grid resolution[a]	0.8 dB	normal	1	1	0.8 dB	0.84 – 1.20	∞
Absorbing boundary conditions[b]	0.0 dB	normal	1	1	0.0 dB	1.00	∞
Tissue parameters fetus[c]	0.01 dB	normal	1	1	0.01 dB	1.00	∞
Simulation time[b]	0.0 dB	normal	1	1	0.0 dB	1.00	∞
Tissue parameters mother[c]	2.5 dB	normal	1	1	2.5 dB	0.56 – 1.8	∞
Amniotic fluid[c]	0.0 dB	normal	1	1	0.0 dB	1.00	∞
SAR Averaging[d]	0.2 dB	normal	1	1	0.2 dB	0.95 – 1.05	∞
Power budget[e]	0.2 dB	normal	1	1	0.2 dB	0.96 – 1.04	∞
Combined std. uncertainty			RSS		2.6 dB	0.55 – 1.80	
Expanded uncertainty *(k_p = 2)*					**4.2 dB**	0.38 – 2.60	

[a]The grid resolution in the fetus is varied between 0.75 mm and 1.0 mm. Due to the grid topology, these changes also affect the resolution of the mother model. The maximum deviation is reported.

[b]The impact of the simulated time and the spurious reflections of the absorbing boundary conditions was assessed by extending thetime by a quarter period and increasing the distance to the boundaries by a quarter wavelength according to the recommendations of IEEE (2008). It is negligible for the settings and configurations used here.

[c]The uncertainty due to the age dependence of the tissue parameters was assessed by replacing the dielectric parameters for the tissue of the unborn, as discussed in section 3.2, by the parameters of the Cole-Cole model. In order to estimate the impact of the parameters of the tissue of the mother, the layer of fat and subcutaneous tissue of the mother's abdomen in the model in the 7thgestational month was replaced by muscle tissue, which has a significantly higher permittivity and conductivity. For the assessmentof the impact of the attenuation in the amniotic fluid, its conductivity was increased by 15 %.

[d]For the fetus models, the SAR averaging uncertainty is based on the difference in body mass of the three-month-old model. Here, the 10 g value could not be assessed for technical reasons. The uncertainty can be estimated conservatively by assuming that the entire power is absorbed in a fraction of the body with a mass of 10 g. For the other cases, it is assessed on the basis of the maximum tolerance of the averaging volume as specified in IEEE (2002).

[e]The power budget is the ratio of the sum of the radiated and absorbed powers to the power fed into the computational domain. For plane wave exposure, the power fed into the computational domain cannot be determined. It has therefore been estimated based on simulations with known source power (Christ et al. 2009).

Table A4. Numerical uncertainty and variability of the local RF exposure of the mother.

Uncertainty source	Tolerance	Distrib.	Div.	*ci*	Std. unc.	Conf. interval	*veff*
Num. uncertainty (Table A3)	2.6 dB	normal	1	1	2.6 dB	0.55 – 1.80	∞
Device representation[a]	0.25 dB	normal	1	1	0.25 dB	0.95 – 1.06	∞
Position of source and fetus[b]	2.8 dB	normal	1	1	2.8 dB	0.53 – 1.90	15
Combined std. uncertainty		RSS			3.4 dB	0.45 – 2.20	
Expanded uncertainty *(k_p = 2)*					**5.3 dB**	0.29 – 3.40	

[a]The device representation is based on the variability of the field decay reported in Kanda et al. (2004) for a large set of different devices.

[b]The positioning uncertainty was assessed using the standard deviation of the local exposure as evaluated above.

Copyright © 2014 Health Physics Society. Unauthorized reproduction of this article is prohibited.

Table A5. Numerical uncertainty of the mother for whole body RF exposure.

Uncertainty source	Tolerance	Distrib.	Div.	*ci*	Std. unc.	Conf. interval	*veff*
Grid resolution[a]	0.0 dB	normal	1	1	0.0 dB	1.0	∞
Absorbing boundary conditions[b]	0.0 dB	normal	1	1	0.0 dB	1.0	∞
Tissue parameters fetus[c]	0.0 dB	normal	1	1	0.0 dB	1.0	∞
Simulation time[b]	0.0 dB	normal	1	1	0.0 dB	1.0	∞
Tissue parameters mother[c]	0.5 dB	normal	1	1	0.5 dB	0.89 – 1.13	∞
Amniotic fluid[c]	0.0 dB	normal	1	1	0.0 dB	1.00	∞
Resonance frequency[d]	0.1 dB	normal	1	1	0.1 dB	0.98 – 1.02	∞
Power budget[e]	0.2 dB	normal	1	1	0.2 dB	0.96 – 1.04	∞
Combined std. uncertainty		RSS			0.6 dB	0.88 – 1.14	
Expanded uncertainty *(k_p = 2)*					**1.1 dB**	0.78 – 1.30	

[a]The grid resolution in the fetus is varied between 0.75 mm and 1.0 mm. Due to the grid topology, these changes also affect the resolution of the mother model. The maximum deviation is reported.

[b]The impact of the simulated time and the spurious reflections of the absorbing boundary conditions was assessed by extending the time by a quarter period and increasing the distance to the boundaries by a quarter wavelength according to the recommendations of IEEE (2008). It is negligible for the settings and configurations used here.

[c]The uncertainty due to the age dependence of the tissue parameters was assessed by replacing the dielectric parameters for the tissue of the unborn, as discussed in section 3.2, by the parameters of the Cole-Cole model. In order to estimate the impact of the parameters of the tissue of the mother, the layer of fat and subcutaneous tissue of the mother's abdomen in the model in the 7th gestational month was replaced by muscle tissue, which has a significantly higher permittivity and conductivity. For the assessment of the impact of the attenuation in the amniotic fluid, its conductivity was increased by 15 %.

[d]For the fetus models, the SAR averaging uncertainty is based on the difference in body mass of the three-month-old model. Here, the 10 g value could not be assessed for technical reasons. The uncertainty can be estimated conservatively by assuming that the entire power is absorbed in a fraction of the body with a mass of 10 g. For the other cases, it is assessed on the basis of the maximum tolerance of the averaging volume as specified in IEEE (2002).

[e]The power budget is the ratio of the sum of the radiated and absorbed powers to the power fed into the computational domain. For plane wave exposure, the power fed into the computational domain cannot be determined. It has therefore been estimated based on simulations with known source power (Christ et al. 2009).

Table A6. Numerical uncertainty of the fetus for whole body RF exposure.

Uncertainty source	Tolerance	Distrib.	Div.	*ci*	Std. unc.	Conf. interval	*veff*
Grid resolution[a]	0.01 dB	normal	1	1	0.01 dB	1.0	∞
Absorbing boundary conditions[b]	0.0 dB	normal	1	1	0.0 dB	1.0	∞
Tissue parameters fetus[c]	0.3 dB	normal	1	1	0.30 dB	0.93 – 1.07	∞
Simulation time[b]	0.01 dB	normal	1	1	0.01 dB	1.0	∞
Tissue parameters mother[c]	1.8 dB	normal	1	1	1.80 dB	0.66 – 1.50	∞
Amniotic fluid[c]	0.15 dB	normal	1	1	0.15 dB	0.97 – 1.03	∞
Resonance frequency[d]	0.1 dB	normal	1	1	0.10 dB	0.98 – 1.02	∞
Power budget[e]	0.2 dB	normal	1	1	0.20 dB	0.96 – 1.04	∞
Combined std. uncertainty		RSS			1.90 dB	0.65 – 1.50	
Expanded uncertainty *(k_p = 2)*					**3.2 dB**	0.48 – 2.10	

[a]The grid resolution in the fetus is varied between 0.75 mm and 1.0 mm. Due to the grid topology, these changes also affect the resolution of the mother model. The maximum deviation is reported.

[b]The impact of the simulated time and the spurious reflections of the absorbing boundary conditions was assessed by extending the time by a quarter period and increasing the distance to the boundaries by a quarter wavelength according to the recommendations of IEEE (2008). It is negligible for the settings and configurations used here.

[c]The uncertainty due to the age dependence of the tissue parameters was assessed by replacing the dielectric parameters for the tissue of the unborn, as discussed in section 3.2, by the parameters of the Cole-Cole model. In order to estimate the impact of the parameters of the tissue of the mother, the layer of fat and subcutaneous tissue of the mother's abdomen in the model in the 7th gestational month was replaced by muscle tissue, which has a significantly higher permittivity and conductivity. For the assessment of the impact of the attenuation in the amniotic fluid, its conductivity was increased by 15 %.

[d]For the fetus models, the SAR averaging uncertainty is based on the difference in body mass of the three-month-old model. Here, the 10 g value could not be assessed for technical reasons. The uncertainty can be estimated conservatively by assuming that the entire power is absorbed in a fraction of the body with a mass of 10 g. For the other cases, it is assessed on the basis of the maximum tolerance of the averaging volume as specified in IEEE (2002).

[e]The power budget is the ratio of the sum of the radiated and absorbed powers to the power fed into the computational domain. For plane wave exposure, the power fed into the computational domain cannot be determined. It has therefore been estimated based on simulations with known source power (Christ et al. 2009).

Copyright © 2014 Health Physics Society. Unauthorized reproduction of this article is prohibited.